Cell Death and Differentiation (2000) 7, 712–720

www.nature.com/cdd

Radiation-induced apoptosis in the adult central nervous system is p53-dependent

BM Chow[1], Y-Q Li[1] and CS Wong*[,1,2]

[1] Division of Experimental Therapeutics, Ontario Cancer Institute, Department of Medical Biophysics, University of Toronto, Toronto, Canada
[2] Department of Radiation Oncology, Princess Margaret Hospital, University Health Network, University of Toronto, Toronto, Canada
* Corresponding author: CS Wong, Princess Margaret Hospital, University Health Network, 610 University Avenue, Toronto, Ontario, M5G 2M9 Canada. Tel: (416) 946-2125; Fax: (416) 946-4586; E-mail: Shun.Wong@rmp.uhn.on.ca

Received 24.6.99; revised 29.2.00; accepted 4.4.00
Edited by FD Miller

Abstract

Oligodendrocytes and subependymal cells in the adult CNS have been shown to undergo radiation-induced apoptosis. Here, we examined the role of p53 in radiation-induced apoptosis in the adult mouse CNS. In the spinal cord of *p53*+/+ mice, apoptotic glial cells were observed within 24 h after irradiation, and the apoptotic response peaked at 8 h. These apoptotic cells demonstrated the immunohistochemical phenotype of oligodendrocytes, and decreased oligodendrocyte density was observed at 24 h after 22 Gy. A similar time course of radiation-induced apoptosis was seen in subependymal cells in the adult mouse brain. Radiation-induced apoptosis was preceded by an increase in nuclear p53 expression in glial cells of the spinal cord and subependymal cells of the brain. There was no evidence of radiation-induced apoptosis in the spinal cord and subependymal region of *p53*−/− animals. We conclude that the p53 pathway may be a mechanism through which DNA damage induces apoptosis in the adult CNS. *Cell Death and Differentiation* (2000) **7,** 712–720.

Keywords: apoptosis; p53; oligodendrocytes; subependyma; radiation

Abbreviations: AEC, 3-amino-9-ethylcarbazole; AI, apoptotic incidence; CNS, central nervous system; DAPI, 4,6 diamidino-2-phenylindole; DIG, digoxigenin; FITC, fluorescein isothiocynate; GC, galactocerebroside; GFAP, glial fibrillary acidic protein; H&E, hematoxylin and eosin; HRP, horseradish peroxidase; IL-2, interleukin-2; plp, proteolipid protein; TUNEL, terminal dUTP nicked end labelling; XRT, ionizing radiation

Introduction

Numerous agents, including chemotherapeutic drugs, oxidative stress and ionizing radiation (XRT) may induce apoptosis. The mechanism of apoptosis appears to be dependent on many factors, including the nature of apoptotic stimuli, cell type and the microenvironment. XRT-induced apoptosis has been observed in a number of cell types, including thymocytes,[1] intestinal crypt cells[2,3] and cerebellar neurons.[4,5]

Oligodendrocytes have been shown to undergo XRT-induced apoptosis *in vitro*[6] and *in vivo* in the rat spinal cord.[7,8] Subependymal cells have also been shown to undergo XRT-induced apoptosis.[9,10] Oligodendrocytes are post-mitotic cells that ensheath neuronal axons with concentric layers of myelin. Myelinated axons conduct much faster than bare axons and demyelination is associated with many neuropathologic conditions. Subependymal cells are cells adjacent to the ventricles of the brain. The function of these cells is largely unknown, but they have been observed to undergo proliferation in response to injury and can give rise to neuronal and non-neuronal cell populations.[11]

The tumour suppressor gene, *p53*, plays a role in XRT-induced apoptosis in thymocytes[1,12] and intestinal crypt cells.[3] A delayed p53-independent apoptosis after XRT however has also been observed in intestinal epithelial cells,[2] and XRT-induced apoptosis in pulmonary endothelial cells was described to be p53-independent.[13] Certain cells of the central nervous system (CNS) have been reported to undergo p53-dependent apoptosis. *In vitro*, post-mitotic cerebellar neurons undergo p53-dependent apoptosis following some DNA damaging agents, including XRT.[4] Cultured oligodendrocytes have been shown to undergo p53-dependent apoptosis following treatment with an interleukin-2 (IL-2) dimer.[14] In the developing CNS, cerebellar granule cells underwent XRT-induced apoptosis, but XRT failed to induce apoptosis in the cerebellum of *p53* null mice.[15]

The role of p53 in XRT-induced apoptosis in the adult CNS has not been described. In this study, we showed evidence for upregulation of the p53 protein in the CNS of *p53* wild-type (+/+) animals after XRT. Adult mice that were null (−/−) for the *p53* gene demonstrated an absence of XRT-induced apoptosis in oligodendrocytes and subependymal cells. We conclude that the p53 pathway may be a mechanism through which DNA-damage response induces apoptosis in the adult CNS.

Results

XRT-induced apoptosis in the spinal cord

To characterise XRT-induced apoptosis in the adult mouse spinal cord (wild-type for *p53*), the cervical segment of the spinal cord (C2 to T2) was given a single dose of 8, 22 or 30 Gy. At different time points, up to 24 h after XRT, apoptosis was assessed morphologically using hematoxylin and eosin (H&E) stain, or biochemically using the terminal dUTP nicked end labelling (TUNEL) assay. TUNEL-stained sections were

also counterstained with the fluorescent nuclear stain, 4,6 diamidino-2-phenylindole (DAPI).

There was no evidence of any gross histopathology in the spinal cord during the 24 h following XRT. The tissue architecture was similar in irradiated and non-irradiated tissues. All blood vessels appeared normal and there was no evidence of inflammation in the irradiated spinal cord.

There was little evidence of apoptosis in the non-irradiated mouse spinal cord. Apoptotic glial cells were observed within the first 24 h after XRT (Figure 1A–C). Morphologically, there was no evidence of apoptosis in neurons or vascular endothelial cells. These apoptotic cells were scattered singly and randomly throughout white and gray matter.

The apoptotic incidence (AI) in the non-irradiated spinal cord, as quantified using morphological criteria in H&E-stained sections, was very low ($0.024 \pm 0.009\%$). A significant increase in AI was observed by 6 h after 22 Gy ($P < 0.05$) compared to non-irradiated wild-type animals (Figure 2). The peak apoptotic response was observed at 8 h and the AI returned to baseline levels by 16 h after 22 Gy (Figure 2). There was no evidence of an increase in AI beyond a single dose of 22 Gy (Figure 3).

The astrocyte-specific marker, glial fibrillary acidic protein (GFAP);[16] oligodendrocyte-specific markers, galactocerebroside[17] (GC) and Leu-7;[18] neuronal marker, synaptophysin;[19] and endothelial cell marker, factor VIII-related antigen,[20] were used to identify the apoptotic cell

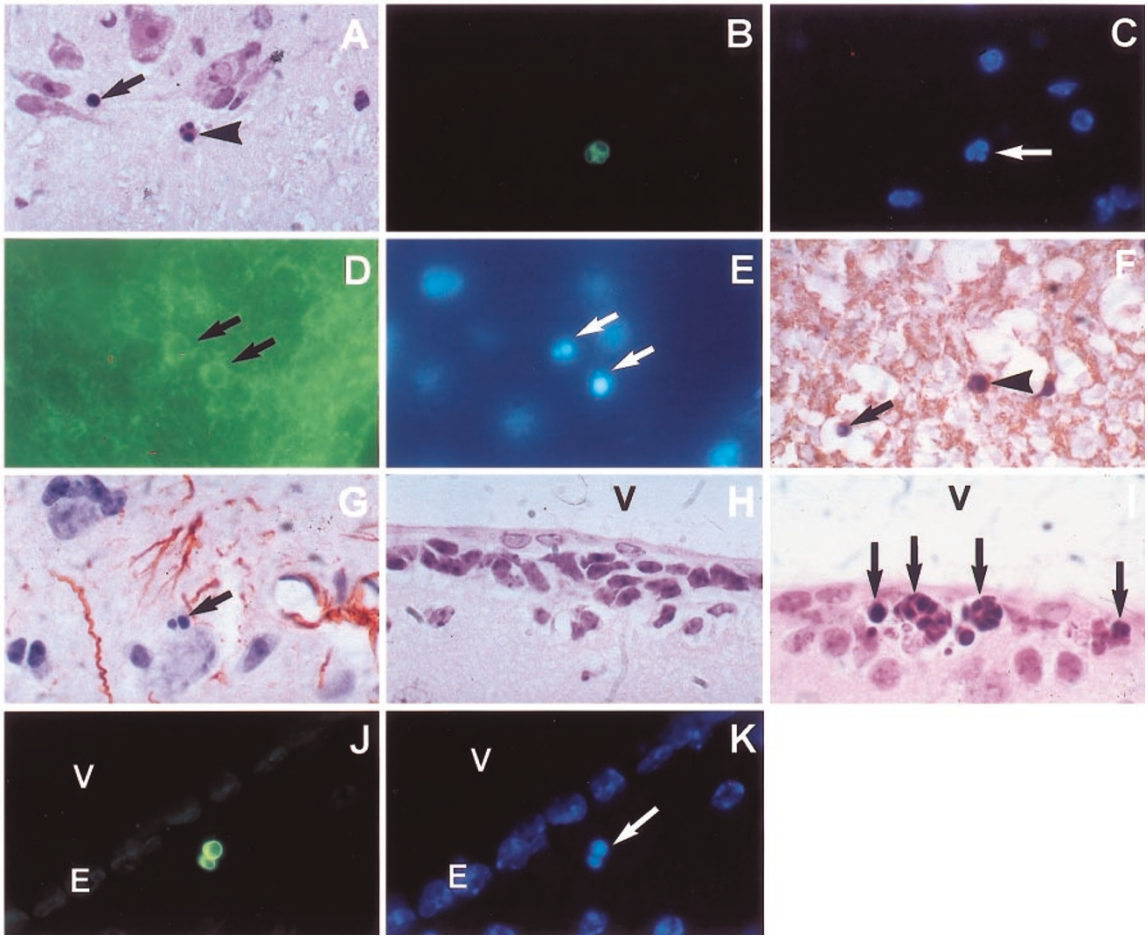

Figure 1 Adult mice wild-type for *p53* were given a single dose of 22 Gy to the spinal cord or 2 Gy to the brain, and sacrificed at different times up to 36 h after XRT. Apoptosis was assessed by H&E staining or TUNEL assay. At 10 h after 22 Gy (**A**), one apoptotic cell (arrow) shows evidence of nuclear condensation and cell shrinkage, while a second apoptotic cell (arrowhead) shown nuclear fragmentation (H&E). At 6 h after 22 Gy in a TUNEL-stained section (**B**), a brightly fluorescent TUNEL positive apoptotic cell also shows morphological evidence of nuclear fragmentation, which is also seen when the sections are counterstained with DAPI (arrow, **C**). Immunohistochemistry on spinal cord sections for the oligodendrocyte-specific marker, GC, demonstrates two apoptotic cells (arrows, **D**) completely surrounded by GC immunoreactivity at 8 h after 22 Gy. The apoptotic cells (arrows, **E**) demonstrate nuclear condensation and fragmentation upon counterstaining with DAPI. Immunohistochemical staining for the oligodendrocyte-specific marker, Leu-7, at 8 h after 22 Gy is observed in an apoptotic cell (arrowhead, **F**) that also demonstrates nuclear fragmentation. Another Leu-7 positive apoptotic cell shows nuclear condensation (arrow, **F**). Immunohistochemistry on spinal cord sections for the astrocyte-specific marker, GFAP, demonstrates that apoptotic cells at 8 h after 22 Gy were negative for GFAP. The location of this GFAP negative apoptotic cell (arrow, **G**) suggests that it is most likely a perineuronal satellite oligodendrocyte. A non-irradiated section of the subependymal region shows no evidence of apoptosis (H&E, **H**). At 6 h after 2 Gy, clusters of apoptotic cells (arrows, **I**) show evidence of cell shrinkage, nuclear fragmentation and eosinophilic cytoplasm. At 6 h after 2 Gy, a brightly fluorescent TUNEL-positive apoptotic subependymal cell (**J**) shows morphological evidence of nuclear fragmentation, which is also seen when the section is counterstained with DAPI (arrow, **K**). Original magnifications $\times 1000$. V, ventricle; E, ependymal cells

type. Apoptotic cells that were completely surrounded by immunoreactivity were considered positive. Most of the apoptotic cells (84.6±5.3%) observed at 8 h after 22 Gy were GC positive (Figure 1D,E), and almost half (48.6±18.6%) of the apoptotic cells were Leu-7 positive (Figure 1F). None of the apoptotic cells were positive for GFAP (Figure 1G), synaptophysin or factor VIII-related antigen (data not shown). Omission of the primary antibodies resulted in no staining, confirming the specificity of the immunohistochemistry.

XRT-induced apoptosis in the subependyma

To examine XRT-induced apoptosis in the subependymal regions, adult p53+/+ mice were given a single dose of 2 Gy to the whole brain. At different time points, up to 36 h after irradiation, tissues were fixed, embedded in paraffin and sectioned at the level of the optic chiasm. Apoptosis was assessed morphologically using H&E-stained sections, or using TUNEL-stained sections counterstained with DAPI.

The non-irradiated subependymal region of adult *p53*+/+ animals (Figure 1H) showed a low incidence of spontaneous apoptosis (0.33±0.02%). Unlike the scattered distribution of apoptotic cells within the spinal cord, clusters of apoptotic cells were often observed in the irradiated subependymal region (Figure 1I). There was no evidence of apoptosis in ependymal cells. As in the irradiated spinal cord, apoptotic subependymal cells also possessed the biochemical hallmarks of apoptosis, as demonstrated by positive TUNEL reactivity (Figure 1J,K). Using morphological criteria in H&E-stained sections to quantify the apoptotic response, peak AI was reached at 4 h after 2 Gy (11.5±1.0%), $P<0.05$ compared to non-irradiated animals. By 24 h, AI decreased to baseline levels (Figure 4).

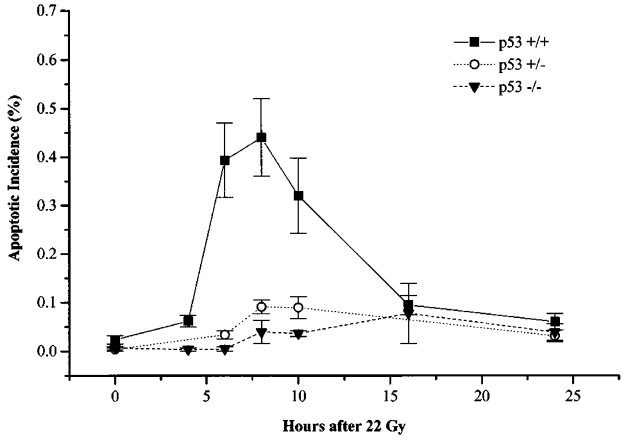

Figure 2 The time course of XRT-induced apoptosis in spinal cords of adult *p53*+/+, +/− and −/− mice after a single dose of 22 Gy was assessed using morphological criteria with H&E staining up to 24 h after irradiation. Three *p53*+/+, +/− and −/− animals were used for all time points, with the exception of 0, 6, 10 and 24 h, where six, seven, four and six *p53*+/+ animals were used respectively. Vertical bars are S.E.M.

Absence of XRT-induced apoptosis in *p53*−/− CNS

To examine the role of p53 in XRT-induced apoptosis in the adult CNS, the apoptotic response in the brain and spinal cord of adult mice heterozygous (+/−) and null (−/−) for the *p53* gene were compared to that in the wild-type animals. In *p53*−/− spinal cord, there was no evidence of XRT-induced apoptosis. Values for AI at the different time points after XRT were not significantly different compared with the corresponding AI in the unirradiated animals (Figure 2).

There was a suggestion of an intermediate response in the spinal cord of *p53*+/− animals. However, AI values for the different time points after XRT did not rise significantly above baseline levels (Figure 2).

There was also no evidence of XRT-induced apoptosis in the subependymal region of adult *p53*−/− animals (Figure 4). The apoptotic response in the *p53*+/− animals

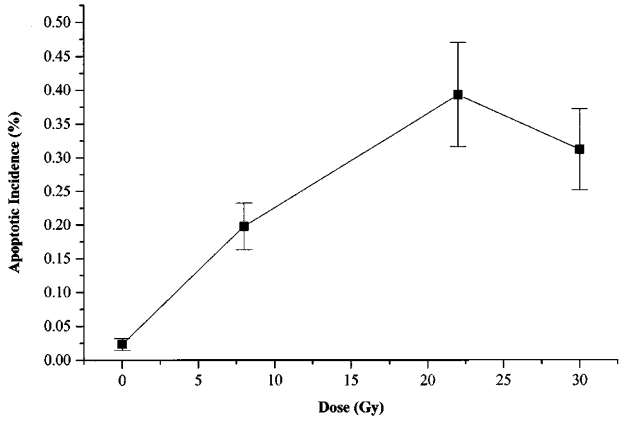

Figure 3 Dose response for XRT-induced apoptosis in the *p53*+/+ mouse spinal cord was assessed using morphological criteria with H&E staining at 6 h after doses of 8, 22 and 30 Gy. Six, three, seven and three animals were used at 0, 8, 22 and 30 Gy respectively. Vertical bars are S.E.M.

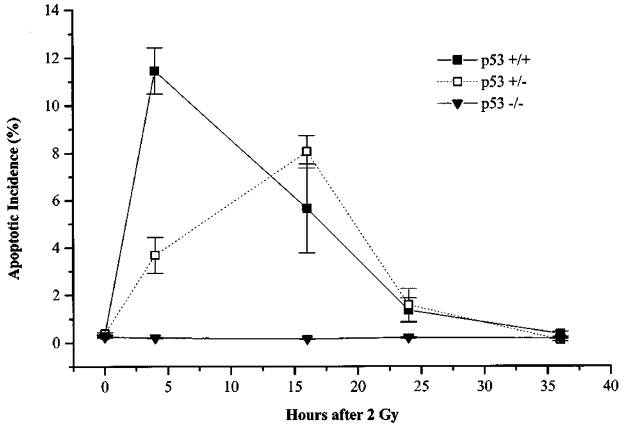

Figure 4 The time course of XRT-induced apoptosis in the subependymal region of adult *p53*+/+, +/− and −/− mice after a single dose of 2 Gy was assessed using morphological criteria with H&E staining at 0, 4, 16, 24 and 36 h after irradiation. Three *p53*+/+, +/− and −/− animals were used for all time points. Vertical bars are S.E.M.

appeared intermediate or delayed compared to that found in *p53*+/+ and −/− animals. Value for AI in the *p53*+/− animals at 4 h after 2 Gy was not significantly different from that in *p53*−/− animals, but was significantly different from the AI in the wild-type mice. At 16 h after 2 Gy, AI in *p53* +/− animals was significantly different from that of the *p53* −/− animals, but not significantly different from that of *p53*+/+ animals.

p53 immunohistochemistry

To determine if the p53 protein is upregulated in the adult CNS following XRT, spinal cord and brain sections from irradiated and non-irradiated wild-type animals were processed for p53 immunohistochemistry. In the non-irradiated spinal cord, only the occasional glial cells of the spinal cord demonstrated p53 immunoreactivity (Figure 5A–C). However, by 4 h following a single dose of 22 Gy to the spinal cord, there was a significant increase in the per cent glial cells that demonstrated nuclear immunostaining for p53 (Table 1, Figure 5D). There was also a slight increase in p53 immunoreactivity in the neuropil. Glial cells in both white (Figure 5E) and gray matter (Figure 5F) showed nuclear p53 immunoreactivity. In gray matter, there were also some neurons that demonstrated p53 immunoreactivity after XRT (Figure 5F).

In the non-irradiated brain, cells in the choroid plexus showed moderate cytoplasmic p53 immunoreactivity, while the ependymal cells were weakly p53 positive (Figure 5G). Subependymal cells did not demonstrate any p53 immunoreactivity (Table 1, Figure 5H). At 4 h after 2 Gy, there was an increase in the per cent p53 immunopositive cells in the subependymal region (Table 1, Figure 5I,J).

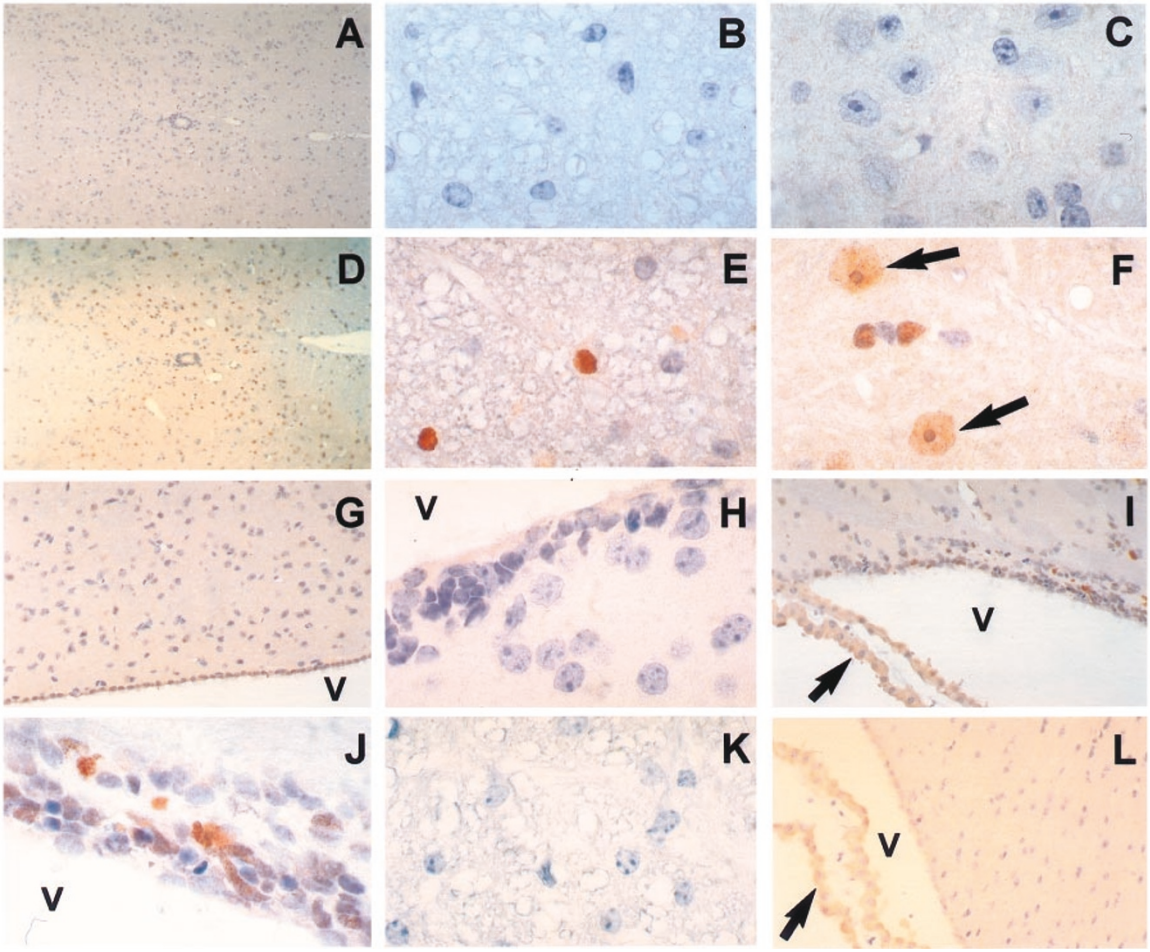

Figure 5 Upregulation of p53 protein after XRT in the CNS of *p53*+/+ animals by immunohistochemistry. There are virtually no p53 immunopositive cells in the non-irradiated spinal cord (**A**, original magnifications ×100; **B**, white matter, ×1000; **C**, gray matter, ×1000). At 4 h after a single dose of 22 Gy, many cells demonstrate p53 immunoreactivity in the nucleus although there is also a slight increase in p53 immunoreactivity in the neuropil (**D**, original magnifications ×100; **E**, white matter, ×1000; **F**, gray matter, ×1000). Most p53 positive cells appear to be glial cells (**E**), while some have morphological characteristics of neurons (arrows, **F**). Nuclei immunoreactive for p53 are intensely stained with a red-brown chromogen. The non-irradiated brain shows p53 immunoreactivity in ependymal cells (**G**, original magnification ×250), but no evidence of p53 immunoreactivity in the subependymal region (**H**, original magnification ×1000). At 4 h after 2 Gy, many p53 positive cells are seen in the subependymal region (**I**, original magnifications ×250; **J**, ×1000). Cells of the choroid plexus (arrow, **I**) show moderate p53 staining in the cytoplasm before and after irradiation. Immunohistochemistry for p53 in the spinal cord of *p53*−/− animals at 4 h after 22 Gy demonstrates no staining (**K**, original magnification ×1000). The non-irradiated choroid plexus (arrow, **I**) of *p53*−/− animals shows moderate cytoplasmic staining suggesting that p53 staining in the choroid plexus is non-specific (**L**, original magnification ×250). V, ventricle

Table 1 Per cent glial nuclei in adult mouse subependyma and spinal cord showing p53 immunoreactivity after XRT

		Per cent p53 positive glial nuclei[a]
Subependyma	Non-irradiated	0.23±0.1%
	4 h after 2 Gy	15.7±2.8%
Spinal cord	Non-irradiated	0.07±0.14%
	4 h after 22 Gy	21.2±2.5%
	8 h after 22 Gy	12.9±2.4%

[a]Mean±S.E.M. of three animals

Table 2 Density of *plp* mRNA positive cells in the adult mouse and rat spinal cord after XRT[a]

		No. of *plp* mRNA positive cells/0.016 mm^2	
	XRT[b]	White matter	Gray matter
Mouse spinal cord	Non-irradiated	9.2±0.6	5.0±0.4
	22 Gy	8.0±0.6	4.0±0.2[c]
Rat spinal cord	Non-irradiated	14.1±0.7	5.9±0.3
	8 Gy	12.2±0.6	5.7±0.3
	22 Gy	10.4±0.5[c]	2.4±0.3[c]

[a]Mean±S.E.M. of three animals. [b]*plp* mRNA positive cell density was assessed at 24 h after irradiation and in non-irradiated age-matched controls. [c]$P<0.05$, compared to non-irradiated controls

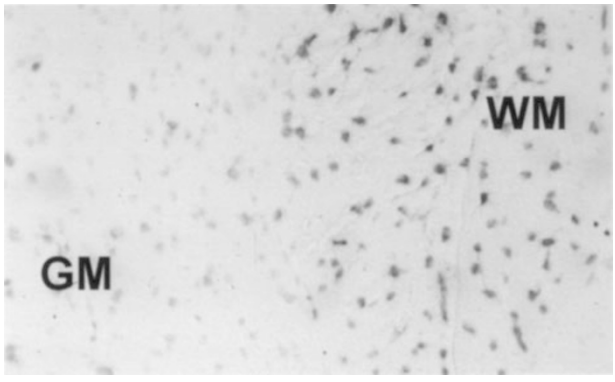

Figure 6 *In situ* hybridization for *plp* mRNA was performed on spinal cord sections from non-irradiated and irradiated (24 h after 22 Gy) *p53*+/+ animals in order to determine if oligodendrocyte cell density changed following XRT. GM, gray matter; WM, white matter. Original magnification ×250

Most of the p53 immunoreactivity appeared to be located in the nucleus of subependymal cells (Figure 5J). In the choroid plexus, the intensity and subcellular localization of p53 staining remained unchanged following XRT (Figure 5J).

Sections of the irradiated small bowel, obtained at 3 h after 8 Gy, demonstrated p53 immunoreactivity only in the crypt cells as previously reported,[2,3] indicating specific staining for p53. Omission of the p53 primary antibody resulted in no specific staining by the secondary antibody. Immunostaining for p53 from *p53*−/− animals demonstrated no staining in the non-irradiated and irradiated (Figure 5K) spinal cord. The choroid plexus of *p53*−/− animals showed moderate cytoplasmic staining and similar intensity of immunoreactivity compared to that in *p53*+/+ animals. These observations suggested that p53 staining in the choroid plexus was non-specific (Figure 5L).

Oligodendrocyte cell density

Since the number of apoptotic oligodendrocytes returned to baseline by 24 h after XRT, oligodendrocyte density was quantified before and at 24 h after XRT to determine if XRT-induced apoptosis is associated with a depletion of the oligodendrocyte population in the wild-type mouse spinal cord. Oligodendrocytes were identified using *in situ* hybridization for mRNA of proteolipid protein (plp), a major myelin-associated protein.[21] There was a decrease (P=0.023) in the density of *plp* mRNA positive cells in gray matter at 24 h after 22 Gy, but the reduction in white matter was not significant (P=0.17, Table 2) compared to non-irradiated age-matched controls.

Since the number of apoptotic cells induced by XRT in the adult mouse spinal cord was small, the rat cervical spinal cord was used to determine if XRT-induced apoptosis is associated with a depletion of the oligodendroglial population. The cervical (C2 to T2) spinal cord of the young adult rat (10-week-old) was irradiated with a single dose of 8 or 22 Gy, and the number of *plp* mRNA positive cells before and at 24 h after XRT was counted. A decrease in the density of *plp* mRNA positive cells was observed after 22 Gy in both white and gray matter compared to non-irradiated age-matched controls. No significant change in the density of *plp* mRNA positive cells in white or gray matter was observed after 8 Gy compared to controls (Table 2).

Discussion

In this study, we used *p53*+/+, +/− and −/− mice to investigate the role of the *p53* tumour suppressor gene in XRT-induced apoptosis in the adult CNS. An apoptotic response was observed in oligodendrocytes and subependymal cells in the adult mouse CNS similar to that reported previously in the adult rat CNS.[7,8,10] The lack of an apoptotic response in *p53*−/− mice following XRT suggests that p53 is required for XRT-induced apoptosis in the adult mouse CNS. To our knowledge, this is the first study that describes the involvement of p53 in XRT-induced apoptosis in the adult CNS *in vivo*.

The time course of XRT-induced apoptosis in the spinal cord and the subependymal region of *p53*+/+ mice was similar to results previously observed in the adult rat CNS.[7,8,10] The peak apoptotic response in the subependymal region of *p53* wild-type mice appeared earlier than that observed in the rat, and the peak AI lower in the mouse compared to the rat. These differences may be due to species-specific responses to XRT, or differences in the definition of the subependymal region. In the present study, a dose-response for XRT-induced apoptosis in the mouse spinal cord was observed. This observation was similar to the results we reported previously in the rat spinal cord.[8]

Immunohistochemical staining using Leu-7, GC, synaptophysin, factor VIII-related antigen and GFAP was in agreement with those in our rat spinal cord studies,[7,8]

suggesting that most of the apoptotic cells observed after XRT in the mouse spinal cord are likely to be cells of the oligodendroglial lineage. Differentiated oligodendrocytes cultured from the neonatal rat brain have also been shown to undergo XRT-induced apoptosis.[6]

To determine if radiation-induced apoptosis was associated with a decrease in oligodendrocyte density of the spinal cord, *in situ* hybridization for *plp* mRNA was performed to identify oligodendrocytes. A decrease in density of *plp* mRNA positive cells was observed after 22 Gy in the rat spinal cord, and in gray matter of the mouse spinal cord. The lack of statistical significance for the decrease in white matter of the mouse spinal cord could simply be due to the smaller number of oligodendrocytes in the mouse spinal cord sections compared to that in the rat.

In the developing mouse CNS, upregulation of p53 coincided with apoptosis after XRT.[22] In E17-18 rat brain, upregulation of p53 protein was reported at 1–3 h after 4 Gy.[23] To assess if XRT-induced apoptosis in the adult mouse CNS is associated with p53 protein upregulation, we performed p53 immunohistochemistry on irradiated and non-irradiated spinal cord and brain sections. A significant increase in p53 expression in glial and subependymal cells following XRT was observed. Consistent with the dependence of XRT-induced apoptosis in p53, increased expression of p53 accumulation was observed at 4 h in the spinal cord, preceding the peak AI observed at 8 h after XRT. A similar pattern of increased p53 expression prior to apoptosis has been observed in intestinal crypt cells[3] and thymocytes following XRT.[1,12]

In the spinal cord, we have not identified the cell type(s) that showed p53 upregulation, but oligodendrocytes are candidate cells. Cultured oligodendrocytes demonstrated nuclear accumulation of p53 after an apoptosis-inducing treatment of dimerized IL-2.[14] Translocation of p53 from the cytosolic to the nuclear compartment was observed recently in oligodendroglia-like cells following hydrogen peroxide treatment.[24] Accumulation of p53 is associated with transcriptional activation of pro-apoptotic genes downstream of p53, such as insulin-like growth factor binding protein 3 and bax.[25,26] Accumulation of p53 triggered by DNA strand breaks can be induced by a number of agents, including XRT. Free radicals have been implicated as the causative agent in p53 upregulation and subsequent apoptosis of cerebellar neurons following XRT.[15] The present results are thus consistent with the mechanism, whereby DNA damage, free radical production and p53 nuclear accumulation lead to apoptosis, in oligodendrocytes and subependymal cells following XRT.

A very low level of apoptosis was observed in the non-irradiated *p53*−/− mouse CNS, implying that the mechanism of spontaneous apoptosis may be p53-independent. A low physiological incidence of p53-independent apoptosis has also been observed in neurons[15] and thymocytes.[1,12] A low level of p53-independent apoptosis is consistent with the general absence of developmental abnormalities in the CNS of *p53*−/− mice,[27] although an increased incidence of neural tube defects was reported in *p53*−/− mice.[28]

In thymocytes and intestinal crypt cells, the apoptotic response following XRT in *p53*+/− mice was intermediate to that found in *p53*+/+ and −/− mice.[1,3] In our study, mice heterozygous for *p53* showed an intermediate apoptotic response in the subependymal region, implying that there is a gene-dose effect of *p53*. There was a suggestion for an intermediate response in the spinal cord of *p53*+/− mice. The lack of statistical significance is likely due to the low AI observed in the *p53*+/− spinal cord.

Oligodendrocytes *in vitro* undergo p53-dependent apoptosis following IL-2.[14] Post-mitotic neurons cultured from neonatal mouse brain undergo p53-dependent apoptosis following XRT.[4,15] However, other pathways of stress-induced apoptosis do exist in the CNS. Activation of c-Jun N-terminal kinase in primary cultures of rat astrocytes, oligodendrocytes and an oligodendrocyte progenitor cell line, CG4, in response to cytokines and other stress inducers has been described.[29] Oligodendrocytes also undergo apoptotic death in response to ceramide treatment.[30–32] Thus, oligodendrocytes and neurons die of apoptosis after a variety of stress-induced stimuli and insults. The role of p53 in these apoptotic pathways has remained uncertain. Recently, evidence for endothelial cell apoptosis was reported in the mouse spinal cord after a very high dose of 50 Gy, and the acid sphingomyelinase-ceramide pathway was implicated in the apoptotic response.[33] In the present study, we failed to identify any evidence of endothelial cell apoptosis after XRT. Although p53 may play a role in some apoptotic pathways, clearly other mechanisms of apoptosis exist in the CNS, and the mechanism by which cells of the developing and adult CNS undergo apoptosis is likely to depend on the nature of the apoptosis-inducing stimulus as well as the cell type.

XRT-induced apoptosis in the developing CNS has been shown to be p53-dependent.[22,23] In this study, we showed that XRT-induced apoptosis in oligodendrocytes and subependymal cells in the adult CNS, and that this process was p53-dependent. Oligodendrocytes are post-mitotic cells, whereas subependymal cells are proliferating cells in the adult CNS.[10] Taken together, these results suggest that apoptosis in both proliferating and post-mitotic cells in the CNS induced by radiation damage is mediated by the p53 pathway.

Materials and Methods

Animals

Adult female *p53*+/+, +/− and −/− mice, 57–123 days old, of the C57BL6/J strain (Jackson Laboratories), and young adult (70-day-old) female Fisher F344 rats (Harlan Sprague Dawley) were used in this study. Genotype of p53 animals was performed by PCR of DNA extracted from blood collected by retro-orbital bleeds. The animals were housed with food and water freely available, and with lighting between 0600 and 1800 h in the animal colony of the Ontario Cancer Institute, an animal colony accredited by the Canadian Council of Animal Care.

Irradiation

Animals were anaesthetized with 3.5% halothane prior to immobilization in a plastic jig. Irradiations were carried out using two Picker

Gemini 100 kV X-ray units employed in a parallel, opposed configuration. Port films to confirm the accuracy of field placement were performed prior to irradiation. Animals were given a single dose of 2 Gy (to the entire brain) or 8, 22, or 30 Gy (to a 1 cm length of C2-T2 of the mouse spinal cord), and sacrificed at various time points up to 36 h after XRT. For the rat experiment, a 2 cm length of the cervical spinal cord (C2-T2) was irradiated. Details of irradiation and dosimetry were previously described.[34] Control animals were not irradiated.

Histopathology

Animals were given an injection of 1 cc of 10% somnotol intraperitoneally. Following transcardiac perfusion using 10% neutral buffered formalin, the cervical portion of the spinal cord (C2-T2) was dissected free of bone and fixed in formalin overnight before embedding in paraffin. Transverse sections, 4 μm thick, were cut from the middle of the spinal cord and stained with H&E or processed for immunohistochemical studies. Controls and animals irradiated to the whole brain were processed similarly. Coronal sections of the brain, 4 μm thick, were cut at the level of the optic chiasm, fixed, embedded, sectioned and stained in the same manner as the spinal cord.

Assessment of apoptosis

Apoptosis in the brain and the spinal cord of *p53*+/+, +/− and −/− animals was assessed morphologically and biochemically using the TUNEL assay.[35] For the morphological assessment of apoptosis, H&E-stained brain and spinal cord sections were used. Criteria for an apoptotic cell included: cell shrinkage with eosinophilic cytoplasm and nuclear condensation or nuclear fragmentation, as described previously.[7,8]

Apoptosis was assessed biochemically using the In Situ Death Detection Kit, Fluorescein (Boehringer Mannheim), which was based on the method of Gavrieli *et al*.[35] Unstained paraffin sections of the brain or spinal cord were deparaffinized, rehydrated and digested with proteinase K (Sigma). 3′OH ends of nicked DNA were tagged with digoxigenin (DIG)-dUTP using terminal deoxynucleotidyl transferase. The tagged ends were labelled with an antibody conjugated to fluorescein isothiocynate (FITC). Sections were dual stained with DAPI (Sigma) using methods described previously.[36]

The AI was obtained for each time point. In the spinal cord, AI was defined as the per cent apoptotic glial cells per transverse section of the spinal cord. For the brain, it was the per cent apoptotic cells per subependymal cells in the subependyma, defined as a 4–5 cell layer thick region surrounding the lateral ventricles. Apoptotic cells were identified using morphological criteria in H&E-stained sections as previously described.[7] For the spinal cord experiments, three *p53*+/+, +/− and −/− animals were used for all time points, with the exception of 0, 6, 10 and 24 h, where 6, 7, 4 and 6 *p53*+/+ animals were used respectively. For the brain experiments, three *p53*+/+, +/− and −/− animals were used for all time points. At least three sections of the brain or spinal cord were scored for each animal. The scoring was performed by an observer (BMC) blinded to the treatment each animal had received.

Sections from the same mouse were averaged to obtain one single mean for each mouse at each time point. All data represented the mean calculated from each mouse at each time point, and the S.E.M. was derived from the mean value from each mouse. Using Dunn's Test, a non-parametric test, each group of animals at each time point was compared with the group of non-irradiated wild-type animals to determine if the AI rose above baseline levels. In addition, Dunn's test was used to determine if the AI at each time point was significantly different in each of the three different p53 genotypes.

Characterization of cell type(s) undergoing apoptosis

To characterize the cell type(s) undergoing apoptosis in the spinal cord, immunohistochemistry studies were done using Leu-7, GC, GFAP, synaptophysin and factor VIII-related antigen as specific markers for oligodendrocyte, astrocytes, neurons and endothelial cells. For GFAP and Leu-7 immunohistochemistry, sections were deparaffinized and endogenous peroxidase activity was blocked by H_2O_2. Methods for immunostaining were similar to those described previously.[8] Briefly for Leu-7 immunohistochemistry, sections were sequentially incubated with anti-Leu-7 antibody (Becton Dickinson, clone HNK-1, 1 : 100), biotinylated anti-mouse IgM and streptavidin horseradish peroxidase (HRP). The reaction was visualized using 3-amino-9-ethylcarbazole (AEC). For GFAP immunostaining, sections were sequentially incubated with anti-GFAP antibody (DAKO), biotin goat anti-mouse IgM, streptavidin-HRP complex and AEC. Factor VIII-related antigen immunohistochemistry was performed using a rabbit polyclonal anti-factor VIII antibody (Dako) in 1/1000 dilution, and sequential incubation with biotin-conjugated with anti-rabbit IgG (Vector Lab), streptavidin-HRP (Dakopatts Corp), and 3, 3′-diaminobenzidine. Synaptophysin immunohistochemistry was performed similarly using 1/400 dilution for the primary antibody. All slides were counterstained with hematoxylin.

At least three different sections from three different animals at 8 h after 22 Gy were used to quantify the per cent GFAP, Leu-7, synaptophysin or factor VIII-related antigen positive apoptotic cells. Apoptotic cells were considered positive if immunoreactivity completely surrounded the piknotic nucleus or nuclear fragments.

The spinal cord of three animals was irradiated separately with a dose of 22 Gy for GC immunohistochemistry. These animals were sacrificed at 8 h after XRT, perfused with 2% paraformaldehyde for 10 min, and the dissected spinal cords were post-fixed for 5 days at 4°C in 2% paraformaldehyde prior to GC immunohistochemistry as described previously.[37] Cryosections were incubated with 0.3 mg/ml $NaBH_4$ in PBS to reduce aldehyde bonds and allow antibody access to antigen. This was followed by incubation with the primary antibody (5 μg/ml; Boehringer Mannheim) and then with FITC-conjugated goat anti-mouse IgG secondary antibody (Boehringer Mannheim), diluted 1 : 200 in PBS containing 0.1% bovine serum albumin. Sections were dual stained with DAPI (Sigma) to identify apoptotic nuclei. The per cent GC positive apoptotic cells from nine spinal sections was recorded. Apoptotic cells were considered positive if immunoreactivity for GC completely surrounded the piknotic nucleus or nuclear fragments counterstained with DAPI.

p53 immunohistochemistry

For p53 immunohistochemistry, sections were deparaffinized, rehydrated, and blocked in 3% H_2O_2. Antigen retrieval was performed by microwaving sections in a 0.01 M citrate buffer (pH 6). Sections were then sequentially incubated in anti-p53 antibody (Nova Castra, clone CM5, 1 : 1000), biotin anti-rabbit IgG, and streptavidin-HRP. The reaction was visualized with AEC and counterstained with hematoxylin. Sections of the mouse small bowel, obtained at 3 h after 8 Gy, were used as a positive control.[2,3] The p53 primary antibody was omitted as a negative control. Spinal cord and brain sections from *p53*−/− mice were stained with the p53 antibody, as described above, to determine the specificity of staining.

Cells were considered p53 positive only if strong p53 immunoreactivity was found in the entire nucleus. The percentage of p53 positive cells in the spinal cord was taken as a per cent of all the glial cells in the transverse spinal cord section. The subependyma was again defined as the region of cells, 4 – 5 cell layers thick, surrounding the lateral ventricles. In the spinal cord, three sections per animal from three mice were counted. In the brain, six sections per animal from at least three mice were counted.

Oligodendrocyte density after XRT

The *plp* mRNA was used as a specific marker for oligodendrocytes[21] to determine if apoptosis in the spinal cord was associated with a decrease in oligodendroglial cell density. The cDNA encoding plp was donated by Dr. Griffiths. The cDNA fragment was cut out by digesting the pGEM3 plasmid containing *plp* cDNA with *Eco*RI and *Hind*III and subcloned into pGEM-4Z vector (Promega). The plasmid carrying a 450 base pair of fragment of the *plp* cDNA coding sequence was linearized with *Eco*RI or *Hind*III (Boehringer Mannheim). The DIG-labelled sense and antisense RNA probes were obtained by *in vitro* transcription with T7 or SP6 RNA polymerase in the presence of DIG-UTP using a DIG RNA labelling kit (Boehringer Mannheim), according to manufacturer's instructions.

The *in situ* hybridization procedure was performed using a modification of a protocol in the Nonradioactive *In Situ* Hybridization Application Manual (Boehringer Mannheim). Briefly, the slides were fixed in 4% paraformaldehyde in PBS, and treated with 0.2 N HCl and proteinase K. The sections were acetylated in freshly prepared 0.5% acetic anhydride in 0.1 M triethanolamine-HCl pH 8.0. The slides were hybridized with DIG-labelled sense or anti-sense probes (100 ng/100 μl) in hybridization buffer (50% formamide, 2 $\times$ SSC, 10% dextran sulfate, 0.01% sheared salmon sperm DNA, and 0.02% SDS). Hybridization was performed at 70°C, followed by a post-hybridization wash in 50% deionized formamide in 1 $\times$ SSC at 55°C. The slides were equilibrated in 1 $\times$ SSC and blocked in blocking mixture (0.1 M Tris pH 7.5, 0.05 M NaCl, 0.2% Tween 20, 10% foetal bovine serum and 1% blocking reagent, Boehringer Mannheim). The slides were then incubated with anti-DIG antibody conjugated with alkaline phosphatase (Boehringer Mannheim), diluted 1:500 in blocking mixture. Visualization of the *plp* mRNA message was done by incubating sections in 5-bromo-4-chloro-3-indolyl phosphate and nitroblue tetrazolium. Slides were counterstained with methyl green (Sigma). The sense probe was used on sections as a negative control, and showed no staining.

Because the number of apoptotic cells returned to control level by 24 h after XRT,[7,8] the impact of XRT-induced apoptosis was evaluated by comparing the number of *plp* mRNA positive cells at 24 h with control. Transverse sections of non-irradiated and irradiated *p53*+/+ mouse spinal cords (24 h after 22 Gy) and rat spinal cords (24 h after 8 or 22 Gy) were used in the analysis.

Five representative areas, each of 0.016 mm^2 per spinal cord section, were selected for the scoring. The cell density in white matter was defined as the mean value in dorsal, lateral, and ventral white matter, and the density in gray matter was the mean of the values for dorsal and ventral gray matter. Three spinal cord sections per animal, and three animals per dose group were assessed. The number of *plp* mRNA positive cells was counted by an observer (YQL) blinded to the treatment. Significant differences were determined by one-tailed Student's *t*-test.

References

1. Lowe SW, Schmitt EM, Smith SW, Osborne BA and Jacks T (1993) p53 is required for radiation-induced apoptosis in mouse thymocytes. Nature 362: 847 – 849
2. Merritt AJ, Allen TD, Potten CS and Hickman JA (1997) Apoptosis in small intestinal epithelial from p53-null mice: evidence for a delayed, p53-independent G2/M-associated cell death after gamma-irradiation. Oncogene 14: 2759 – 2766
3. Merritt AJ, Potten CS, Kemp CJ, Hickman JA, Balmain A, Lane DP and Hall PA (1994) The role of p53 in spontaneous and radiation-induced apoptosis in the gastrointestinal tract of normal and p53-deficient mice. Cancer Res. 54: 614 – 617
4. Enokido Y, Araki T, Tanaka K, Aizawa S and Hatanaka H (1996) Involvement of p53 in DNA strand break-induced apoptosis in postmitotic CNS neurons. Eur. J. Neurosci. 8: 1812 – 1821
5. Kim SH, Chung CY and Son CH (1998) Cell death by apoptosis in the neonatal mouse cerebellum following gamma-irradiation. Anticancer Res. 18: 1629 – 1632
6. Vrdoljak E, Bill CA, Stephens LC, Van der Kogel AJ, Ang KK and Tofilon PJ (1992) Radiation-induced apoptosis of oligodendrocytes *in vivo*. Int. J. Radiat. Biol. 62: 475 – 480
7. Li YQ, Guo YP, Jay V, Stewart PA and Wong CS (1996) Time course of radiation-induced apoptosis in the adult rat spinal cord. Radiother. Oncol. 39: 35 – 42
8. Li YQ, Jay V and Wong CS (1996) Oligodendrocytes in the adult rat spinal cord undergo radiation-induced apoptosis. Cancer Res. 56: 5417 – 5422
9. Bellinzona M, Gobbel GT, Shinohara C and Fike JR (1996) Apoptosis is induced in the subependyma of young adult rats by ionizing irradiation. Neurosci. Lett. 208: 163 – 166
10. Shinohara C, Gobbel GT, Lamborn KR, Yamada E and Fike JR (1997) Apoptosis in the subependyma of young adult rats after single and fractionated doses of X-rays. Cancer Res. 57: 2694 – 2702
11. Goldman SA, Zukhar A, Barami K, Mikawa T and Niedzwiecki D (1996) Ependymal/subependymal zone cells of postnatal and adult songbird brain generate both neurons and nonneuronal siblings in vitro and in vivo. J. Neurobiol. 30: 505 – 520
12. Clarke AR, Purdie CA, Harrison DJ, Morris RG, Bird CC, Hooper ML and Wyllie AH (1993) Thymocyte apoptosis induced by p53-dependent and independent pathways. Nature 362: 849 – 852
13. Santana P, Pena LA, Haimovitz-Friedman A, Martin S, Green D, McLoughlin M, Cordon-Cardo C, Schuchman EH, Fuks Z and Kolesnick R (1996) Acid sphingomyelinase-deficient human lymphoblasts and mice are defective in radiation-induced apoptosis. Cell 86: 189 – 199
14. Eisenberg O, Faber-Ellman A, Gottlieb E, Oren M, Rotter V and Schwartz M (1995) Direct involvement of p53 in programmed cell death of oligodendrocytes. EMBO J. 14: 1136 – 1144
15. Wood KA and Youle RJ (1995) The role of free radicals and p53 in neuron apoptosis in vivo. J. Neurosci. 15: 5851 – 5857
16. Ludwin SK, Kosek JC and Eng LF (1975) The topographical distribution of S-100 and GFA proteins in the adult rat brain: an immunohistochemical study using horse radish peroxidase-labelled antibodies. J. Comp. Neurol. 165: 197 – 208
17. Raff MC, Mirsky R, Fields KL, Lisak RP, Dorfman SH, Silberberg DH, Gregson NA, Leibowitz S and Kennedy MC (1978) Galactocerebroside is a specific cell-surface antigenic marker for oligodendrocytes in culture. Nature 274: 813 – 816
18. Schuller-Petrovic S, Gebhart W, Lassmann H, Rumpold H and Kraft D (1983) A shared antigenic determinant between natural killer cells and nervous tissue. Nature 306: 179 – 181
19. Wiedenmann B and Franke WW (1985) Identification and localization of synaptophysin, an integral membrane glycoprotein of Mr 38,000 characteristic of presynaptic vesicles. Cell 41: 1017 – 1028
20. McComb RD, Jones TR, Pizzo SV and Bigner DD (1982) Specificity and sensitivity of immunohistochemical detection of factor VIII/von Willebrand factor antigen in formalin-fixed paraffin-embedded tissue. J. Histochem. Cytochem. 30: 371 – 377

21. Griffiths IR, Schneider A, Anderson J and Nave KA (1995) Transgenic and natural mouse models of proteolipid protein (PLP)- related dysmyelination and demyelination. Brain Pathol. 5: 275 – 281
22. Herzog KH, Chong MJ, Kapsetaki M, Morgan JI and McKinnon PJ (1998) Requirement for Atm in ionizing radiation-induced cell death in the developing central nervous system. Science 280: 1089 – 1091
23. Borovitskaya AE, Evtushenko VI and Sabol SL (1996) Gamma-radiation-induced cell death in the fetal rat brain possesses molecular characteristics of apoptosis and is associated with specific messenger RNA elevations. Brain Res. Mol. Brain Res. 35: 19 – 30
24. Uberti D, Yavin E, Gil S, Ayasola KR, Goldfinger N and Rotter V (1999) Hydrogen peroxide induces nuclear translocation of p53 and apoptosis in cells of oligodendroglia origin. Brain Res. Mol. Brain Res. 65: 167 – 175
25. Buckbinder L, Talbott R, Velasco-Miguel S, Takenaka I,Faha B, Seizinger BR and Kley N (1995) Induction of the growth inhibitor IGF-binding protein 3 by p53. Nature 377: 646 – 649
26. Miyashita T and Reed JC (1995) Tumor suppressor p53 is a direct transcriptional activator of the human bax gene. Cell 80: 293 – 299
27. Donehower LA, Harvey M, Slagle BL, McArthur MJ, Montgomery Jr CA, Butel JS and Bradley A (1992) Mice deficient for p53 are developmentally normal but susceptible to spontaneous tumours. Nature 356: 215 – 221
28. Sah VP, Attardi LD, Mulligan GJ, Williams BO, Bronson RT and Jacks T (1995) A subset of p53-deficient embryos exhibit exencephaly. Nat. Genet. 10: 175 – 180
29. Zhang P, Miller BS, Rosenzweig SA and Bhat NR (1996) Activation of C-jun N-terminal kinase/stress-activated protein kinase in primary glial cultures. J. Neurosci. Res. 46: 114 – 121
30. Casaccia-Bonnefil P, Aibel L and Chao MV (1996) Central glial and neuronal populations display differential sensitivity to ceramide-dependent cell death. J. Neurosci. Res. 43: 382 – 389
31. Casaccia-Bonnefil P, Carter BD, Dobrowsky RT and Chao MV (1996) Death of oligodendrocytes mediated by the interaction of nerve growth factor with its receptor p75. Nature 383: 716 – 719
32. Larocca JN, Farooq M and Norton WT (1997) Induction of oligodendrocyte apoptosis by C2-ceramide. Neurochem. Res. 22: 529 – 534
33. Pena LA, Fuks Z and Kolesnick RN (2000) Radiation-induced apoptosis of endothelial cells in the murine central nervous system: protection by fibroblast growth factor and sphingomyelinase deficiency. Cancer Res. 60: 321 – 327
34. Wong CS, Minkin S and Hill RP (1992) Linear-quadratic model underestimates sparing effect of small doses per fraction in rat spinal cord. Radiother. Oncol. 23: 176 – 184
35. Gavrieli Y, Sherman Y and Ben-Sasson SA (1992) Identification of programmed cell death *in situ* via specific labelling of nuclear DNA fragmentation. J. Cell Biol. 119: 493 – 501
36. Li YQ and Wong CS (1998) Apoptosis and its relationship with cell proliferation in the irradiated rat spinal cord. Int. J. Radiat. Biol. 74: 405 – 417
37. Ellison JA and de Vellis J (1994) Platelet-derived growth factor receptor is expressed by cells in the early oligodendrocyte lineage. J. Neurosci. Res. 37: 116 – 128.